Evolution of the magnetic order in the Ho(Mn, Al)$_2$ system; neutron diffraction study

2002 J. Phys.: Condens. Matter 14 11737

(http://iopscience.iop.org/0953-8984/14/45/315)

INSTITUTE OF PHYSICS PUBLISHING JOURNAL OF PHYSICS: CONDENSED MATTER

J. Phys.: Condens. Matter **14** (2002) 11737–11745 PII: S0953-8984(02)53464-0

Evolution of the magnetic order in the Ho(Mn, Al)$_2$ system; neutron diffraction study

I V Golosovsky[1,4], I Mirebeau[2], A S Markosyan[3], J Rodriguez-Carvajal[2] and T Roisnel[2]

[1] St Petersburg Nuclear Physics Institute, 188350 Gatchina, St Petersburg, Russia
[2] Laboratory of Léon Brillouin, CE-Saclay, F-91191 Gif-sur-Yvette, Cedex, France
[3] Faculty of Physics, Moscow State University, 119899 Moscow, Russia

E-mail: golosov@mail.pnpi.spb.ru

Received 13 September 2002
Published 1 November 2002
Online at stacks.iop.org/JPhysCM/14/11737

Abstract

The neutron diffraction study of Ho(Mn$_{1-x}$Al$_x$)$_2$ shows the coexistence of two cubic Laves phases with different unit-cell parameters and substantially different magnetic behaviours. The first phase combines ordered ferrimagnetic and disordered antiferromagnetic components of the magnetic moments. With increasing Al content, starting from the long-range ferrimagnetic order with the induced Mn moment in HoMn$_2$, the progressive formation of spontaneous Mn moments yields short-range order, which in turn transforms to ferromagnetic order in HoAl$_2$. The second phase with incommensurate magnetic structure is driven by the spontaneous Mn moments and exists only over limited ranges of Al content and unit-cell parameter. It has a finite correlation length and appears from a second-order transition without a magneto-volume effect.

1. Introduction

Despite the large number of studies on the rare-earth Laves phases RMn$_2$, our understanding of the magnetism in these materials is far from being complete. This is connected with the large number of competing parameters which govern the magnetic behaviour. In addition to the dual character of the magnetic 3d electrons, which can change between itinerant and localized, geometrical frustration [1, 2] plays an important role. Moreover, in these intermetallics the magnetic and structural stability are sensitive to non-stoichiometry, which can also influence the magnetic behaviour.

A possible way to modify the character of 3d electrons in RMn$_2$ is the change the Mn–Mn spacing by replacing, for example, Mn by Al. Such substitution increases Mn–Mn distance and allows one to approach or reach the critical region above which the character of the 3d electrons changes from itinerant to localized [3].

[4] Author to whom any correspondence should be addressed.

Our early experiments with the $Ho(Mn_{1-x}Al_x)_2$ system, performed at a low substitution of Al for Mn only, with $x \leqslant 0.1$, showed unusual features [4]. All samples consisted of two cubic Laves phases with slightly different unit-cell parameters, but with very different magnetic orders.

In the phase with the larger unit-cell parameter a complex magnetic order with long-range ferrimagnetic and short-range antiferromagnetic components was found. The observed short-range order (SRO) was based on the type II antiferromagnetic order in the fcc lattice (hereafter AF2 structure). This phase will be referred to as the *F-phase*. An incommensurate magnetic structure was observed in the phase with the smaller unit-cell parameter. This phase will be referred to as the *I-phase*.

Surprisingly, no sharp magneto-volume effect was observed at low substitution of Al for Mn, suggesting that the threshold of instability had not been reached; while in the related system $Dy(Mn, Al)_2$ with the bigger Mn–Mn spacing, the threshold of instability was observed at small Al content [3].

In the present neutron diffraction study the $Ho(Mn_{1-x}Al_x)_2$ system was investigated over the whole range of Al content, from $HoMn_2$ to $HoAl_2$. This allowed us to study in detail the interplay of two competing effects: the stabilization of Mn moments with the lattice expansion and the weakening of the Mn magnetism with dilution.

Taking these two effects into account, we can explain qualitatively the peculiarities of the observed magnetic phases and the origin of the discrepancy in the magnetic order reported for the $HoMn_2$ by different authors [4–7].

2. Experimental details

The diffractometer G6-1 of the Laboratory Léon Brillouin (LLB) with a neutron wavelength of 4.732 Å was used to study the long-period magnetic structures. To obtain the values of the magnetic moments and occupation factors, additional measurements were carried out on the multicounter diffractometer of the St Petersburg Nuclear Physics Institute and the diffractometer G4-2 of the LLB, with neutron wavelengths of 1.655 and 2.343 Å, respectively. All neutron diffraction patterns were treated by the FullProf program [8]. The magnetic form factors included in this program were used.

Polycrystalline samples of $Ho(Mn_{1-x}Al_x)_2$ were synthesized by standard induction melting. In contrast with other RMn_2 compounds, $HoMn_2$ can crystallize in the cubic or in the hexagonal structure. The cubic phase can be transformed to the hexagonal phase by lengthy annealing. Therefore, to stabilize the cubic structure and to avoid the formation of the hexagonal structure, the synthesis was followed by quenching that limits the phase segregation.

3. Sample characterization

From x-ray and neutron diffraction measurements it was found that the samples with $x \leqslant 0.6$ consist of two cubic Laves phases with close lattice parameters. This phase separation does not depend on the quality of the constituent metals or synthesis. This is not surprising taking into account the different ionic radii of Al and Mn. However, in the related system $Dy(Mn_{1-x}Al_x)_2$ the phase separation was observed for large $x \geqslant 0.1$ only [3], while in $Ho(Mn_{1-x}Al_x)_2$ the phase separation was already observed in $HoMn_2$.

Obviously, the phase separation and the difference in magnetic behaviour of the two phases are closely related to the structural peculiarities. Therefore we performed a careful structural analysis of our samples by means of neutron and x-ray diffraction.

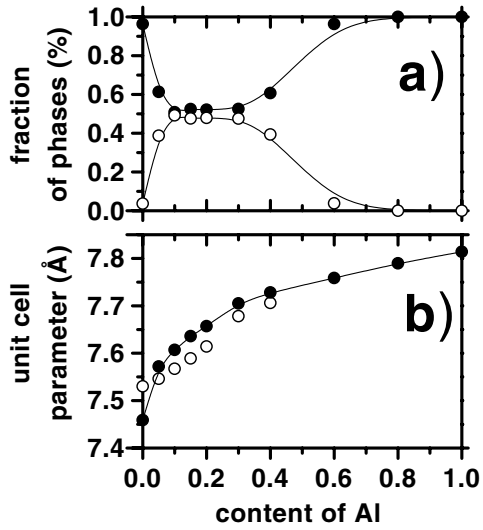

Figure 1. Concentration dependences of the fractions (a) and the unit-cell parameters (b) of two constituent phases: I (open circles) and F (solid circles), measured at low temperature. The errors do not exceed the sizes of the symbols. The solid curves are guides for the eye.

The intensities of the Bragg reflections are proportional to the occupation factors of Ho and Mn sites in the two constituent phases and to the amounts of the phases. Since these parameters are strongly correlated, we could not vary all of them simultaneously and it was necessary to impose some constraints. We considered two alternative models. In the first model, we assumed the same occupation factors for Mn sites, but different occupation factors for Ho sites in the two phases, whereas in the second model we assumed different occupation factors for Mn sites, but the same occupation factor for the Ho sites. These models describe equally well the observed profile and cannot be distinguished by means of powder diffraction.

However, the calculation shows that the second model gives too large a deviation, up to 40%, of the mean Al content from the nominal one, which is nonphysical; therefore this model has to be rejected. The relative amounts and the unit-cell parameters of the two phases, calculated in the framework of the first model with different stoichiometries of Ho in the F-and I-phases, are shown in figure 1.

From the refinement it follows that in the F-phase the occupancy factor for the Ho site is close to unity, while in the I-phase it is markedly lower. One can explain this by a partial occupancy of the Ho site in the I-phase by Mn, which has a negative neutron scattering length. The calculations show that with increasing Al content, up to 25 at.% of Ho in the I-phase can be substituted for Mn. The refinement of x-ray diffraction profiles confirms this result.

The refined occupation factors for the Mn sites appeared to be different from the expected stoichiometric values. This can be explained by the presence of a small amount of Ho at the Mn sites. This value decreases from 4.0(5) at.% in $HoMn_2$ to zero at $x \approx 0.4$.

The non-stoichiometry in the Ho(Mn, Al)$_2$ system leads to observed broadening of the nuclear reflections due to inner strains. This effect had been previously noticed by other authors [5], who suggested that such strains could influence the Mn magnetism. The differences in the stoichiometry, which depends on the sample preparation, explain the differences in the magnetic structures observed by different authors in $HoMn_2$ [4–7].

Also, Ho and Mn atoms partly substitute for one another in the Ho(Mn, Al)$_2$ system—however, in different ways in the two constituent phases. Since the magnetic structures

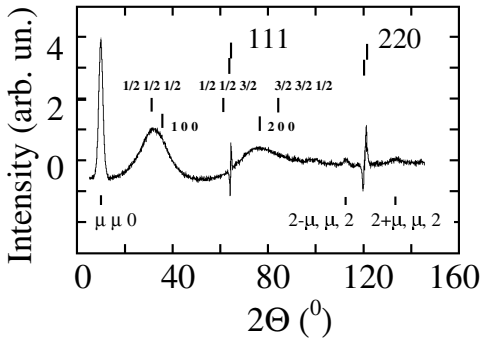

Figure 2. The difference neutron diffraction pattern of $Ho(Mn_{0.6}Al_{0.4})_2$ measured at the diffractometer G6-1 at 10 K. The positions of the nuclear Bragg reflections (the corresponding profiles are omitted), the diffuse maxima with half-integer indexes corresponding to AF2 structure and the maxima corresponding to a primitive lattice are marked by vertical bars. The positions of the satellites are shown at the bottom.

drastically differ in these phases, it seems reasonable to discuss their magnetic behaviours separately.

4. Results and discussion

4.1. Complex magnetic order in the F-phase with short-range antiferromagnetic and long-range ferromagnetic orders

In all samples, including $HoMn_2$, we observed diffuse maxima instead of the superstructure Bragg reflections observed previously in $HoMn_2$ [5], $DyMn_2$ [9] and $TbMn_2$ [10] (figure 2). Ferromagnetic contributions to the nuclear reflections were observed only in the regions of Al concentration $x \leqslant 0.4$ and $x \geqslant 0.8$. This means that the long-range order (LRO) of ferromagnetic (or ferrimagnetic) character is stabilized at low and high Al content only. In the intermediate region, the LRO practically disappears and only the SRO of antiferromagnetic character exists.

The width of the first diffuse peak centred at the node $\frac{1}{2}\frac{1}{2}\frac{1}{2}$ gives an averaged diameter of the magnetic clusters of about 25 Å. This value does not change with temperature and weakly depends on the Al concentration. The temperature dependence of the intensity of the diffuse peak is shown in figure 3 for several Al concentrations. This allows one to determine a temperature T_{SRO} for the onset of the antiferromagnetic SRO. From the temperature dependence of the Bragg peak intensities, one can also determine a temperature T_{LRO} for the occurrence of the ferrimagnetic LRO.

The values of the ordered Mn and Ho moments can be obtained separately by the refining of the magnetic contribution to the nuclear reflections. As regards SRO, one can only determine an average antiferromagnetic component, whose magnitude is proportional to the square root of the intensity of the diffuse scattering.

The analysis shows that both Ho and Mn moments are involved in the SRO as well as in the LRO. In substituted samples all Mn layers, including the frustrated Kagomé-like layer, appeared to be magnetic, in contrast with the 'sandwich'-type structure with a non-magnetic layer, which was reported earlier for the ordered component in $HoMn_2$ [5].

Figure 4 summarizes the evolution of the magnetic order with Al dilution. The disordered moment shows a broad maximum in the region of intermediate Al concentration. At low Al

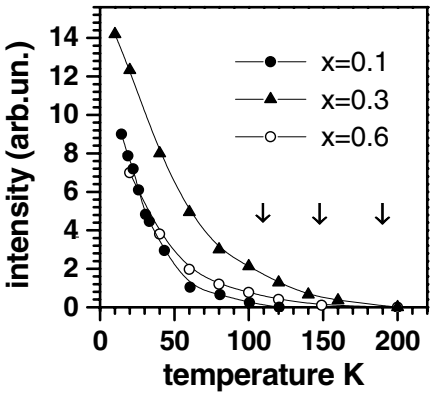

Figure 3. The temperature dependence of the diffuse scattering for $x = 0.1$ (solid circles), 0.3 (triangles) and 0.6 (open circles). The temperatures of onset of the diffuse scattering T_{SRO} are marked by arrows.

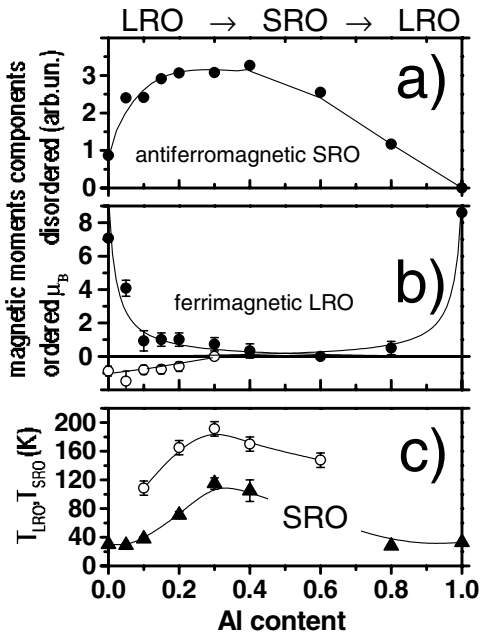

Figure 4. Concentration dependences in the F-phase: (a) the disordered antiferromagnetic component, (b) ordered ferrimagnetic components of Ho (solid circles) and Mn (open circles) moments, (c) temperatures of ordering of ferrimagnetic (T_{LRO}; solid triangles) and antiferromagnetic (T_{SRO}; open circles) components. The errors (e.s.d.) do not exceed the sizes of the symbols, if not shown. The solid lines are guides for the eye.

concentration ($x \leqslant 0.4$), there is ferrimagnetic LRO of Ho and the induced Mn moments as in $HoMn_2$; at high Al content ($x \geqslant 0.8$), there is ferromagnetic LRO of Ho moments only.

The dependences $T_{LRO}(x)$ and $T_{SRO}(x)$ show a surprising feature, namely they go through a maximum with increasing Al content x. Such evolution of the magnetic order can be readily explained by the progressive formation of the local moment in the Mn sites [1, 2], which is responsible for the increase of $T_{LRO}(x)$ and $T_{SRO}(x)$ with increasing Mn–Mn spacing.

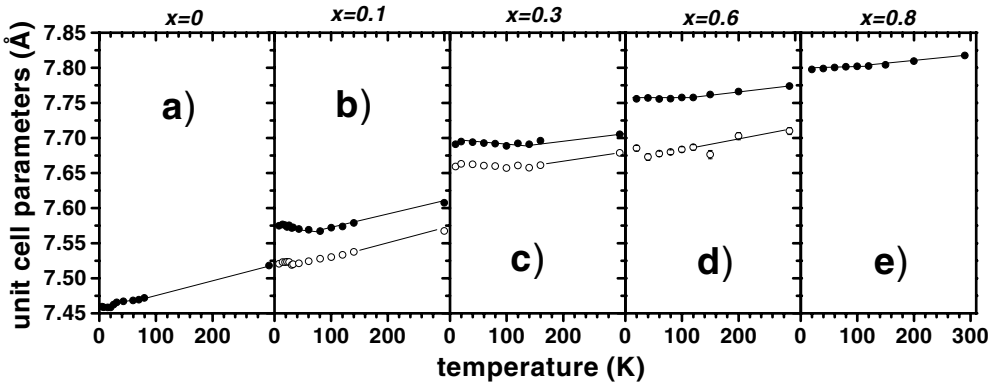

Figure 5. The temperature dependence of the unit-cell parameters in $Ho(Mn_{1-x}Al_x)_2$ for the F-phase (solid circles) and I-phase (open circles). Panels (a)–(e) correspond to Al content $x = 0$, 0.1, 0.3, 0.6 and 0.8, respectively. Errors do not exceed the sizes of the symbols. The solid lines are guides for the eye.

At low Al concentration ($x < 0.4$), the Ho magnetism (namely, ferromagnetic Ho–Ho and antiferromagnetic Ho–Mn interactions) imposes the magnetic order in the F-phase. The rapid reduction of the ordered Ho moments with increasing Al concentration, also observed in magnetization measurements, can be explained by the presence of random molecular fields from the localized Mn moments [2].

At intermediate Al concentration, the large localized Mn moments and frustrated antiferromagnetic Mn–Mn interactions become dominant, yielding breakdown of the long-range magnetic order and making the SRO dominant. Finally, at high Al concentration ($x > 0.8$), the effect of Mn dilution becomes very strong, so Ho moments (and ferromagnetic Ho–Ho interactions) play a dominant role again.

There is unusual coexistence of two mutually perpendicular components of the Mn moment with different character in the F-phase. The ordered ferrimagnetic component of the Mn moment was found, induced by the Ho field, only for $x \leqslant 0.05$. It disappears with increasing Al content. In contrast, the disordered antiferromagnetic component of the Mn moment has a spontaneous character. It starts to increase with Al content increase, then reaches a maximum and finally decreases at high Mn dilution.

This interpretation of Mn magnetism in the F-phase has been confirmed by a recent diffraction experiment on $Ho(Mn_{0.9}Al_{0.1})_2$ under high pressure [11]. It was shown that with increasing pressure, the diffuse maxima gradually transform into Bragg reflections. In fact, an applied pressure destabilizes the frustrated Mn magnetism and, as a result, Ho–Ho interactions become dominant.

The temperature dependence of the lattice unit-cell parameters is shown in figure 5 for several Al concentrations. Although no sharp magneto-volume effect is observed, there is a marked anomaly in the temperature dependence of the unit-cell parameter of the F-phase. A similar anomaly in the thermal expansion curves has been observed previously in the Ho(Mn, $Al)_2$ system and was considered as evidence of the onset of spontaneous Mn moments [2].

4.2. Incommensurate magnetic structure in the I-phase

The I-phase with incommensurate magnetic structure is detected in the concentration range $0 \leqslant x \leqslant 0.6$. Its fraction rapidly increases from 3.7% in $HoMn_2$ to a maximal value of about

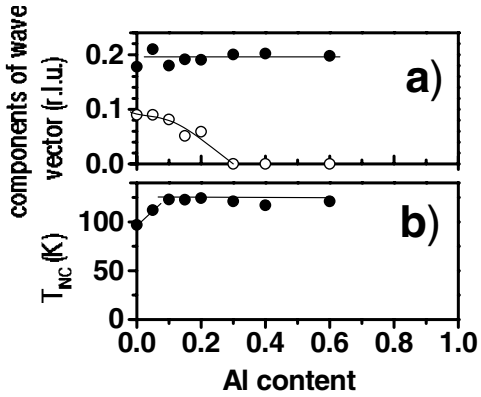

Figure 6. Concentration dependences in the I-phase: (a) components of the wavevector $\boldsymbol{k} = [\mu, \mu, \nu]$: μ (solid circles) and ν (open circles) respectively; (b) the temperature of transition T_{INC}. The errors do not exceed the size of the symbols. The solid curves are guides for the eye.

50% at $x \sim 0.3$ (figure 1). This phase exists only in a narrow interval of the unit-cell parameter 7.53 Å $\leqslant a \leqslant$ 7.71 Å and has disappeared already at a small pressure below 0.9 GPa [11].

Besides the strong diffuse scattering associated with the F-phase, a weak diffuse scattering is also observed in the diffraction spectra, localized around the nodes of the primitive lattice (figure 2). Its temperature dependence scales approximately with the intensity of zero satellite of the incommensurate structure, suggesting that this diffuse scattering should be connected with the I-phase.

The intensity calculation shows that the incommensurate magnetic structure involves both Ho and Mn magnetic moments. With increasing Al content the wavevector transforms from $\boldsymbol{k}_1 = [\mu, \mu, \nu]$ to $\boldsymbol{k}_2 = [\mu, \mu, 0]$ (figure 6(a)) and the magnetic moments in the incommensurate structure rotate with respect to the crystal axes. From the temperature dependence of the zero satellite, one can determine the transition temperature T_{INC} in the I-phase. It is plotted in figure 6(b) versus Al concentration. Besides a weak increase at small Al content, T_{INC} is practically independent of Al concentration.

The T_{INC} of $\sim$120 K is much higher than the ordering temperature in $HoMn_2$ of 31 K, and close to the ordering temperature of spontaneous Mn moments of $\sim$100 K in YMn_2 [12]. The high Néel temperature shows that the magnetic order in the I-phase is driven by the spontaneous Mn moments. However, in contrast to YMn_2, Ho(Mn, Al)$_2$ shows no magneto-volume effect associated with the onset of the incommensurate magnetic structure. Moreover, it appears from a second-order transition rather than the first-order transition observed in YMn_2.

The zero satellite at small angles from the incommensurate magnetic structure was found to be markedly broadened with respect to instrumental resolution. A peak broadening arising from inner strains is proportional to $\tan(\Theta)$ while a broadening due to a finite-size effect is proportional to $1/\cos(\Theta)$. Therefore, the observed broadening at small angles 2Θ should be attributed mainly to a finite-size effect. The evaluation gives an averaged correlation length of about 150 Å. This value, which should be considered a lower limit, does not change with temperature and slightly decreases with increasing Al content. Therefore we suggest that the absence of a cooperative magneto-volume effect and the observation of a second-order transition instead of an expected first-order transition result from a finite correlation length of the incommensurate magnetic structure.

A simple collinear model assuming that the ordered magnetic moments vary with a sinusoidal law describes well the observed intensities of the satellites. The observed weak

diffuse scattering localized around the nodes of the primitive lattice provides the conservation of the total moment. However, this model yields parallel alignment of the Ho and Mn moments in the incommensurate structure, whereas one would expect an antiparallel alignment from the antiferromagnetic R–Mn interaction, typical for Laves phases with the heavy rare earths. Therefore the question of the real structure in the I-phase is still open. The Mn atoms found in the Ho sites could change the local environment, resulting in a sophisticated magnetic order.

5. Conclusions

The neutron diffraction study of $Ho(Mn_{1-x}Al_x)_2$ shows that in this system two cubic Laves phases with complex magnetic behaviour coexist. These phases (I and F) differ in unit-cell parameter, stoichiometry and magnetic behaviour.

In the I-phase, the incommensurate magnetic structure is driven by the spontaneous Mn moments. The fraction of this phase, detected already at a low level (3.7%) in $HoMn_2$, increases to the maximal value of about 50% for an Al concentration $x \sim 0.3$ and goes to zero at $x = 0.6$. In contrast with the incommensurate structures observed in YMn_2 [14], $TbMn_2$ [10] or $GdMn_2$ [13], the incommensurate structure in Ho(Mn, Al)$_2$ appears from a second-order transition and has a finite correlation length of about 150 Å.

The F-phase exists over the whole concentration range and its nature drastically changes with Al concentration. This phase shows a coexistence of the ordered ferrimagnetic and disordered antiferromagnetic components of the moments. Their relative magnitudes change with Al content. Starting from the LRO with the induced Mn moments ($HoMn_2$), the antiferromagnetic SRO driven by the spontaneous Mn moments becomes progressively dominant with increasing Al content. In the intermediate region the LRO disappears. When the Al concentration increases further, the SRO disappears and the ferromagnetic LRO driven by Ho moments is stabilized, like in $HoAl_2$. The change in the magnetic order from LRO to SRO is attributed to the change in the nature of the Mn magnetism, from induced to spontaneous.

How to precisely determine a threshold of instability is not obvious, since the transition from induced to spontaneous Mn moments occurs without any sharp magneto-volume effect. From our measurements, the threshold of instability should be situated around $x \sim 0.05$, which corresponds to Mn–Mn spacing of about 2.68 Å. At this point the anomaly in the temperature dependence of the unit-cell parameter is maximal. There is also a marked change in the concentration dependences of the lattice constant and disordered moment, which increase rapidly below $x = 0.05$ and much more slowly above.

The present study shows that Al substitution leads to the complex magnetic structures in the frustrated Laves phases driven by the spontaneous moments of Mn.

Acknowledgments

The work was supported by RFBR Grants (N-02-02-16981 and N-00-02-17844) and the Russian Federal Foundation for Neutron Studies on Condensed Matter. We are grateful to Dr A Stratilatov for x-ray measurements. One of us (IVG) acknowledges the financial support of the CNRS during his stay in LLB.

References

[1] Shiga M 1988 *Physica* B **149** 293
[2] Shiga M 1994 *J. Magn. Magn. Mater.* **129** 17
[3] Golosovsky I V, Mirebeau I, Markosyan A S, Fischer P and Pomjakushin P 2002 *Phys. Rev.* B **65** 014405

[4] Dubenko I S, Golosovsky I V, Markosyan A S and Mirebeau I 1998 *J. Phys.: Condens. Matter* **10** 11755
[5] Ritter C, Cywinski R, Kilcoyne S H and Mondal S 1992 *J. Phys.: Condens. Matter* **4** 1559
[6] Chamberlain J 1977 *Physica* B **86–88** 138
[7] Hardman K, Rhyne J, Malik S and Wallace W 1982 *J. Appl. Phys.* **53** 1944
[8] Rodriguez-Carvajal J 1993 *Physica* B **55** 902
[9] Ritter C, Kilcoyne S H and Cywinski R 1991 *J. Phys.: Condens. Matter* **3** 727
[10] Brown P, Ouladdiaf B, Ballou R, Deportes J and Markosyan A S 1992 *J. Phys.: Condens. Matter* **4** 1103
[11] Mirebeau I, Goncharenko I N and Golosovsky I V 2001 *Phys. Rev.* B **64** 140401(R)
[12] Gaidukova I Yu and Markosyan A S 1982 *Sov. Phys.–Phys. Met. Metallogr.* **54** 168
[13] Ouladdiaf B, Ritter C, Ballou R and Deportes J 2000 *Physica* B **276–278** 670
[14] Ballou R, Deportes J, Lemaire R, Nakamura Y and Ouladdiaf B 1987 *J. Magn. Magn. Mater.* **70** 129